energies

Article

Solar Resource for Urban Communities in the Baja California Peninsula, Mexico

Alberto-Jesús Perea-Moreno [1,*] and Quetzalcoatl Hernandez-Escobedo [2]

1 Department of Applied Physics, University of Cordoba, CEIA3, Campus de Rabanales, 14071 Córdoba, Spain

2 Faculty of Engineering Campus Coatzacoalcos, University of Veracruz, Harrapa, Veracruz 0052229, Mexico; qhernandez@uv.mx

* Correspondence: aperea@uco.es; Tel.: +34-957-212-632; Fax: +34-957-212-068

Academic Editor: Francisco Manzano Agugliaro
Received: 21 July 2016; Accepted: 27 October 2016; Published: 3 November 2016

Abstract: Several studies have determined that Mexico has great renewable energy potential, and one of its most abundant resources is solar energy, a source that could be exploited to provide development opportunities to its population, however it is necessary to calculate the amount of this source available. The aim of this study was to assess solar irradiance at urban communities in the Baja California Peninsula. For this purpose data recorded every 10 min during 6 years (2010–2015) by the Automatic Meteorological Stations (AMSs) and Synoptic Automatic Meteorological Stations (SAMSs) of the National Meteorological System of Mexico (NMS) were analyzed. Satellite data from the Surface and Meteorology Energy System (SMSE) were also used, and a linear regression was performed to compare the measured and satellite data. The highest R-square value found was 0.97 and the lowest was 0.82. Daily patterns show that Cabo San Lucas had the highest average solar irradiation/day, with 1000 W/m^2. Considering the urban areas, total solar irradiation reaching the Peninsula is about 447 $\times$ 10^6 kWh, which represents around 447 times the total Baja California Peninsula yearly energy consumption. Geographic Information System (GIS) helped to identify the zones and months with higher solar resources. May is the month registering the highest irradiation, more than 8.1 kWh/m^2/day, while the average solar resource for the whole Peninsula is 5.7 kWh/m^2/day.

Keywords: urban communities; solar irradiation; assessment; geographic information system (GIS); Baja California Peninsula

1. Introduction

According to [1] two thirds of world electricity production comes from fossil fuels, followed by hydroelectric plants (16.5%), nuclear plants (10.6%), biofuels and waste (2%), while geothermal, solar, wind and other sources make up the remaining 3.3%. Electricity in Mexico is mainly generated from fossil fuels and Mexico occupies the tenth place in global oil production [2].

However, electricity demand is increasing as well as the resulting environmental problems. Solar photovoltaic (PV) electricity generation plays an important role among the worldwide renewable energy technologies because it is a clean and environmentally friendly source of energy [2]. Since the early 2000s, photovoltaic solar systems have become one of the most popular renewable energy sources in the world and their global market share has grown exponentially [3], driven mainly by industrialized countries like Germany, Japan, Spain and the United States, as well as China. Policy support was largely focused on mitigating the higher costs of PV generation compared to fossil fuels, especially through Feed-In-Tariffs [4]. In the past few years, the market prices and underlying costs of PV systems have shrunk dramatically, which makes PV competitive with fossil fuels in many regions and if existing fossil fuel subsidies were to be reduced, renewables like PV would become even more competitive. PV use has increased 360% from 2010 to 2014, and in some regions installed costs have been reduced by more than a half during the same period [5]. Bloomberg New Energy Finance (BNEF) forecasts that costs will continue to shrink, making solar electricity generation competitive with other conventional sources worldwide by 2026 [6].

On the other hand, PV financing costs have been reduced in many countries and at the same time, experience with solar PV has grown and the subsequent financial risks fallen [7]. Due to the reduction of costs, there is a renewed interest in solar PV in locations with lower solar irradiance, where previously it was considered economically unfeasible.

Investors need to consider if investing in solar PV generation is financially feasible. For a company it is important to identify potential projects that provide added value to the company. Despite the pressure to use renewable energy resources to reduce CO_2 emissions, investors and companies will only invest in this type of sources if it also coincides with the goal of maximizing wealth [8,9].

In Mexico the renewable energy generation mix consists of hydropower (13%), geothermal (8%), wind (0.25%) and solar PV (0.001%) [10]. In 2012 the generation of electricity through solar PV was 2 GWh, which increased to 13 GWh in 2015. In 2008 the energy law was reformed, and now private investors can distribute, transmit and supply energy. Concerning renewables, the share of wind has increased, and its installed capacity is around 3283 MW [11].

In Mexico the solar resource has been assessed in particular regions, and estimates show that in a country where there is an average irradiance of 6.5 kWh/m^2/day [12], almost all this energy to potentially generate electricity is wasted. In Sonora, in northern Mexico, a validation of solar data was done for a numerical weather prediction model to generate a high spatial (9 km) and temporal (10 min) resolution assessment of global solar irradiance [13]. Solar resources were also calculated for states along the Gulf of Mexico, where the highest energy (6.22 kWh/m^2/day) was found in Tamaulipas and the lowest (5.03 kWh/m^2/day) in the state of Veracruz, however, lowest in this case does not mean that it would be useless to generate electricity [12]. The first PV farm was installed in Baja California Sur in 2015, and it is expected to generate 35 MW [10], however, the capacity of this project could be considered low in comparison with the national solar potential. CSP is another alternative for solar energy exploitation, and according to [11] 1,800,000 m^2 of solar collectors were installed in 2012.

All this solar resource could generate electricity that could be exported to the grid or used in stand-alone mode. Some studies indicate that in Mexico 99.6% of urban communities are electrified [14] while others indicate that only 78% of the urban population are electrified [15]. In the Baja California Peninsula the electrification in urban zones is around 97.6%, which represents 3,796,096 people [16].

The gross electric energy generation by the Baja California Peninsula until March 2016 was around 1,179,545 MWh, of which 991,964 MWh were generated by Baja California and 187,580 MWh by Baja California Sur, respectively [17]. Energy policy in Mexico has been modified in recent years, and in 2015, the Energetic Transition Law was published which established that the Ministry of Energy will set the goal of a minimum share of clean energy in power generation at 25% by 2018, 30% by 2021 and 35% by 2024 [18].

The aim of this work was to assess the energy output generated by solar irradiance in urban community areas in the Baja California Peninsula, using GIS to help to identify zones with higher solar resources.

2. Materials and Methods

2.1. Ground Data

The Baja California Peninsula is located in northwest Mexico, bordering to the North with the United States and bounded by the Pacific Ocean to the east and Cortes Sea to the west. The peninsula has two states or provinces: Baja California and Baja California Sur. The first has 853,254 households and the second has 174,441 households, respectively, and between them, urban electrification is around 97.6% (Figure 1).

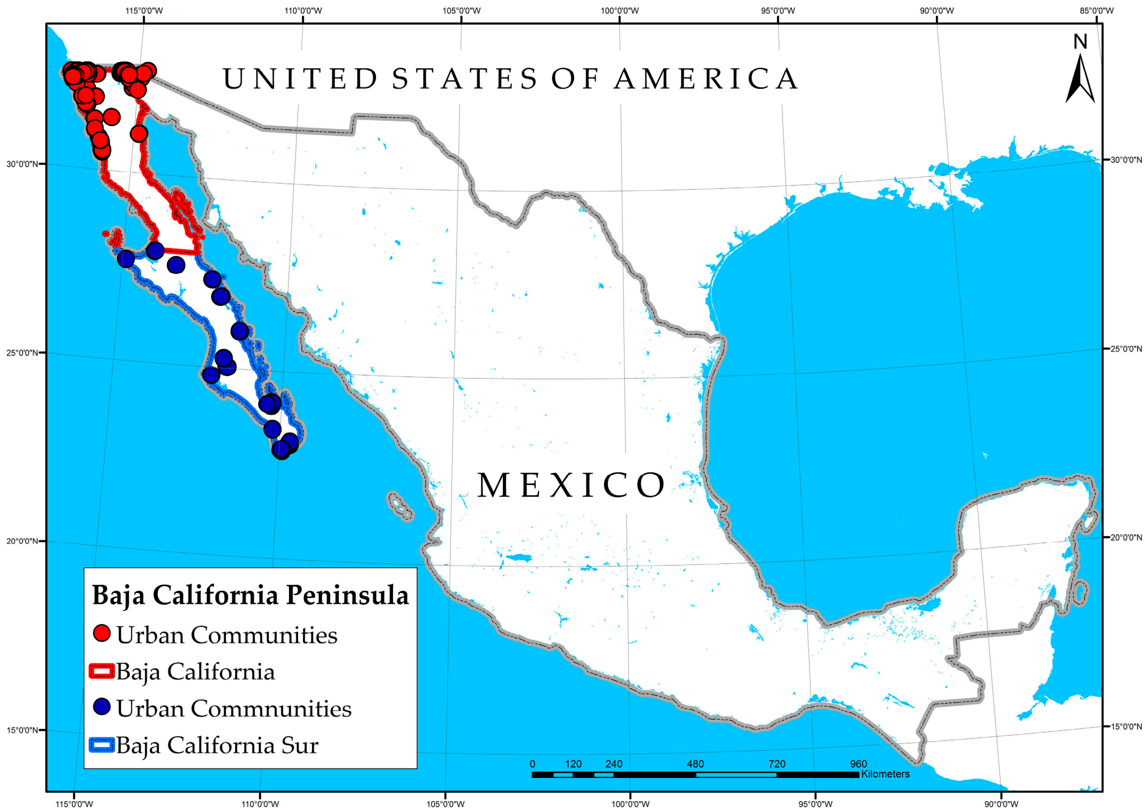

Figure 1. Baja California Peninsula.

Our data analysis consists of determining the relation between the meteorological variable data, such as irradiation (W/m^2), air temperature (°C) and atmospheric pressure (mbar), recorded every 10 min during 6 years, 2010–2015 by 14 AMSs and seven SAMSs from NMS of Mexico [19] with monthly mean satellite data obtained from SMSE [20]. The SMSE data along the peninsula were included to avoid problems in the interpolation model, because as can be observed in Figure 2, the AMSs and SAMSs are not close enough to each other, resulting in coverage gaps. The amount of data represents around 310,000 data points, and the percentage of gaps is 12% because there were months without data.

Due to a lack of pyranometers in the country, SMSE data are used. The solar radiation data given by SMSE is obtained directly or derived from parameters available from the NASA/Global Energy and Water Cycle Experiment—Surface Radiation Budget (NASA/GEWEX SRB) Project Release 3.0, Validation of the solar data is based upon comparisons against research quality observations from the Baseline Surface Radiation Network. Solar parameters are output on a 1° × 1° global grid at 3-hourly temporal resolution for each day of the month, which is equivalent to around 111 km resolution [20]. In spite of the ever-increasing network of meteorological stations around the world, the availability of solar radiation data is still limited for many applications in terms of spatial distribution [21]. Consequently, it is widely accepted that global solar radiation data derived from satellites are an excellent tool for analyzing solar resources and for supplying time series of solar irradiation [22,23]; this application was demonstrated by Pedro and Coimbra [24], who evaluated techniques to prognosticate solar potential using non-exogenous data.

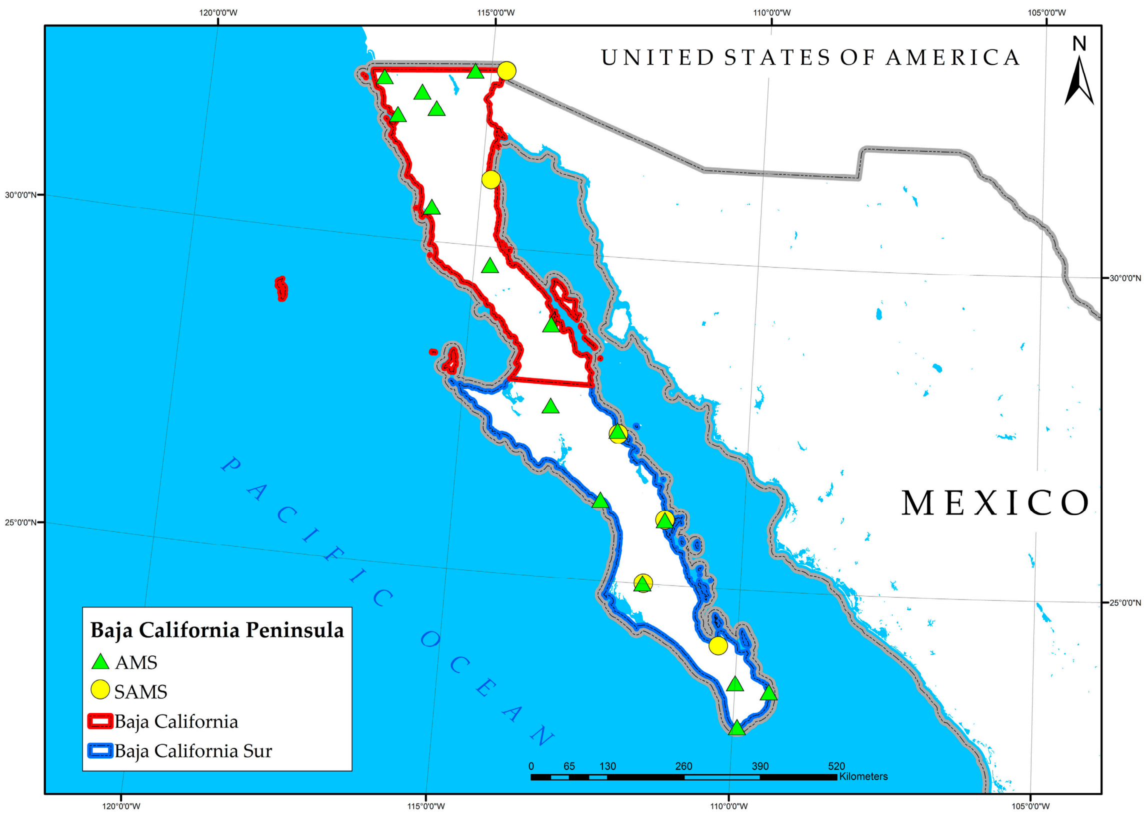

Figure 2. Baja California Peninsula.

Table 1 lists the geographic positions of the AMSs and SAMSs.

Table 1. Meteorological station coordinates along the Baja California Peninsula.

Source	Meteorological Station	State	N (°)	W (°)	Altitude
AMS	Bahia Angeles	Baja California	28.8964	113.5603	10
AMS	Catavina	Baja California	29.7272	114.7192	514
AMS	Const. 1857	Baja California	32.0419	115.9217	1576
AMS	Mexicali	Baja California	32.6669	115.2908	50
AMS	Presa Abelardo L.	Baja California	32.4472	116.9083	156
AMS	Presa Emilio Lo	Baja California	31.8913	116.6033	32
AMS	La Rumorosa	Baja California	32.2722	116.2056	1262
AMS	San Quintin	Baja California	30.5317	115.8375	32
SAMS	Algodones	Baja California	32.7047	114.7303	40
SAMS	Ejido Nvo. Leon	Baja California	32.4128	115.1919	11.4
SAMS	San Felipe	Baja California	31.0281	114.8344	20
AMS	Bahia de Loreto	Baja California Sur	26.0097	111.3539	1
AMS	Cabo Pulmon	Baja California Sur	23.4450	109.4244	25.9
AMS	Gust Diaz Ordaz	Baja California Sur	27.6428	113.4575	37
AMS	San Juanico	Baja California Sur	26.2575	112.4786	36
AMS	Cabo San Lucas	Baja California Sur	22.8811	109.9267	224
AMS	Santa Rosalia	Baja California Sur	27.3381	112.2694	53
AMS	Sierra Laguna	Baja California Sur	23.5553	109.9986	1949
SAMS	Cd Constitucion	Baja California Sur	25.0097	111.6467	48
SAMS	La Paz	Baja California Sur	24.1167	110.3167	18
SAMS	Loreto	Baja California Sur	26.0114	111.3500	15
SAMS	Sta Rosalia	Baja California Sur	27.2833	112.2500	82

2.2. Methods

Data from fixed sensors eventually loses records and time series will be incomplete. To solve this situation a MatLab application, summarized in Figure 3, has been used. Input data are recorded hourly every 10 min, so an hour has six records and a month 4032, 4320 or 4464, respectively, depending on whether it is 28, 30 and 31 days long. Next the application compares the number of data per hour, and if it finds missing data it displays a graph and selects the best gap filling model, e.g., 2 January 2010 has missing data, so this application compares the plots and the best fit is chosen (see Figure 4).

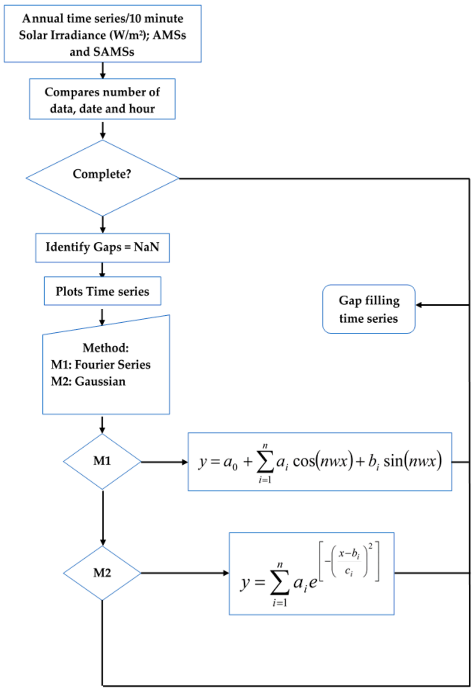

Figure 3. Gap filling algorithm.

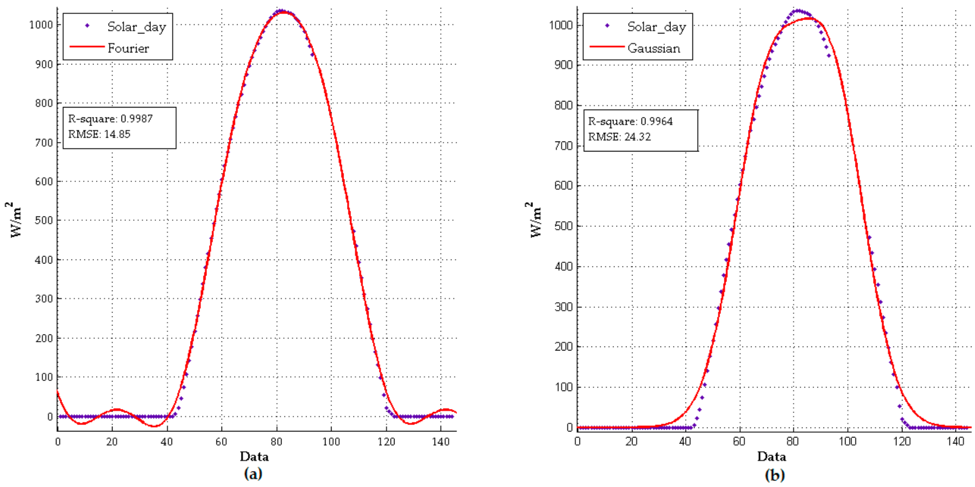

Figure 4. Gap filling. (**a**) A Fourier model and (**b**) A Gaussian model.

Figure 4 illustrates how the application works. In this case two models were used, a Fourier and a Gaussian one, and even though both have an R-square value of 0.99 the Gaussian model does not fit the date well. The Fourier series is a sum of sine and cosine functions that describes a periodic signal. It is represented in either the trigonometric form or the exponential form and is given by Equation (1):

$$y = a_0 + \sum_{i=1}^{n} a_i \cos\left(nwx\right) + b_i \sin\left(nwx\right) \tag{1}$$

where a_0 models a constant (intercept) term in the data and is associated with the i = 0 cosine term, w is the fundamental frequency of the signal, n is the number of terms (harmonics) in the series, and $1 \leq n \leq 8$. Gaussian model: This model fits peaks and is given by Equation (2):

$$y = \sum_{i=1}^{n} a_i e^{\left[-\left(\frac{x-b_i}{c_i}\right)^2\right]} \tag{2}$$

where a is the amplitude, b is the centroid (location), c is related to the peak width, n is the number of peaks to fit, and $1 \leq n \leq 8$.

Data need quality control; statistics are a useful tool for this. R-squared, Root Mean Square Error (*RMSE*) was employed in [25–27], who used these methods to eliminate data errors. A useful statistical measure such as R-squared, also known as coefficient of determination, describes the relationship between a output variable, and one or more input variables and it can be defined as the percentage of the response variable variation that is explained by a linear model, which may be written using Equations (3)–(6):

$$SS_E = \sum_{i=1}^{n} (y_i - \hat{y})^2 \; df_E = n - 2 \tag{3}$$

$$SS_R = \sum_{i=1}^{n} (\hat{y}_1 - \overline{y})^2 = \sum_{i=1}^{n} y_i^2 - n\overline{y}^2 \tag{4}$$

$$SS_T = SS_E + SS_R \tag{5}$$

$$R - square = \frac{SS_R}{SS_T} = 1 - \frac{SS_E}{SS_T} \tag{6}$$

where SS_E is the Error Sum of Squares (Equation (3)), SS_R is the Regression Sum of Squares (Equation (4)) and SS_T is the Total Sum of Squares (Equation (5)). Finally R-square is given by Equation (6). *RMSE*, also termed the standard error of the regression, is given by Equation (7), and is the standard deviation of the residuals:

$$RMSE = \sqrt{\frac{\sum_{i=1}^{n} (y_i - \hat{y}_i)^2}{n}} \tag{7}$$

where $\hat{y}_1$ is the predicted response of observation j from the selected regression. In statistics, the mean absolute error (*MAE*) is a quantity used to measure how close forecasts or predictions are to the eventual outcomes. The mean absolute error is given by Equation (8):

$$MAE = \frac{1}{n} \sum_{i=1}^{n} |y_i - \hat{y}_i| \tag{8}$$

An estimator should be close in some sense to the true value of the unknown parameter. Formally, is can say that $\hat{\theta}$ is an unbiased estimator of θ if the expected value of is equal to $\hat{\theta}$. This is equivalent to saying that the mean of the probability distribution of $\hat{\theta}$ (or the mean of the sampling distribution of $\hat{\theta}$) is equal to θ. The point estimator $\hat{\theta}$ is an unbiased estimator for the parameter if θ, Equation (9):

$$E\left(\hat{\theta}\right) = \theta \tag{9}$$

If the estimator is not unbiased, then the difference is given by Equation (10):

$$E\left(\hat{\theta}\right) - \theta \tag{10}$$

is called the bias of the estimator $\hat{\theta}$. When an estimator is unbiased, the bias is zero; see Equation (11):

$$E\left(\hat{\theta}\right) - \theta = 0 \tag{11}$$

2.3. Typical Meterological Year

Irradiance data were separated monthly to generate a Typical Meteorological Year (TY), which is considered as a single years-worth of hourly data to represent radiation data over a historical period of multiple years. It is necessary to calculate a TMY from each AMSs and SAMSs, TMY is a data set of hourly values of solar radiation and meteorological elements for a 1-year period developed by [28]. It consists of months selected from individual years and concatenated to form a complete year. A TMY provides a standard for hourly data for solar radiation and other meteorological elements that permit performance comparisons of system types and configurations for one or more locations. A TMY represents conditions judged to be typical over a long period of time, such as 30 years. Because they represent typical rather than extreme conditions, they are not suited for designing systems and their components to meet the worst case conditions occurring at a location.

2.4. Solar Resource Maps in the Baja California Peninsula

Higher solar resource zones could be identified spatially with maps designed using ArcGIS gridding solar global irradiance (*Gh*) to produce visually appealing maps from irregularly spaced data. The method applied to interpolate in ArcGIS software was the kriging method, which is based on statistical models that include autocorrelation—that is, the statistical relationships among the measured points. Because of this, geostatistical techniques not only have the capability of producing a prediction surface but also provide some measure of the certainty or accuracy of the predictions. Kriging assumes that the distance or direction between sample points reflects a spatial correlation that can be used to explain variation in the surface, Kriging is given by Equation (12):

$$Z\left(S_0\right) = \sum_{i=1}^{n} \lambda_i Z\left(S_i\right) \tag{12}$$

where n is the number of measured values; λ_i is an unknown weight for the measured value at the ith location; S_i is the the measured value at the ith location and S_0 is the prediction location.

3. Results

3.1. Validation

The comparison process evaluates the quality of data. One problem is the lack of meteorological data, and in this case, we had to use SMSE data, obtained monthly as G_h. AMSs and SAMSs results needed to be calculated monthly as well to identify the relationships between these source, SMSE gives monthly and annual irradiation data; its resolution is low but they were used to help the interpolation. Table 2 presents this statistical analysis.

Table 1 shows that satellite data can be used as a complement to assess solar resources, and these data fitted with the meteorological data, the best fit corresponding to SMSE EjidoNLeon, which has an R-square of 0.97, SSE 0.96154 and *RMSE* 0.31009 kWh/m^2. In general only Catavina AMSs has a higher SSE (6.89759), but it has an R-square of 0.82, which means that it can be used, but it is also biased and has values close to 0, which indicate that the dispersion is from the mean is lower values. To explain the linear regression between meteorological and satellite data were divided by state. Figure 5 shows Baja California and Figure 6 shows Baja California Sur.

Table 2. Statistic parameters of AMSs and SAMSs versus SMSE data.

Source		SS_E	R-Square	*RMSE* kWh/m^2/day	*MAE*	Bias
Bahia Angeles	SMSE_Ban	1.45149	0.95	0.38098	0.16	0.032
Catavina	SMSE_Cat	6.89759	0.82	0.83052	0.29	0.150
Const. 1857	SMSE_C1857	3.17617	0.86	0.56358	0.23	0.082
Mexicali	SMSE_Mex	0.92855	0.97	0.30472	0.14	0.037
Presa Abelardo L	SMSE_PrAbe	1.31309	0.96	0.36237	0.12	0.025
Presa Emilio Lo	SMSE_PEmilio	2.50370	0.89	0.50040	0.14	0.032
La Rumorosa	SMSE_Rum	1.08316	0.97	0.32911	0.21	0.058
San Quintin	SMES_SanQuin	2.21336	0.91	0.47046	0.17	0.051
Algodones	SMSE_Algod	1.36899	0.96	0.37000	0.27	0.089
Ejido Nvo. Leon	SMSE_Ejido	0.96154	0.97	0.31009	0.16	0.052
San Felipe	SMSE_SanFelipe	1.02661	0.96	0.32041	0.23	0.063
Bahia de Loreto	SMSE_BLoreto	1.67932	0.92	0.40980	0.15	0.032
Cabo Pulmon	SMSE_CabP	2.44898	0.84	0.49487	0.24	0.073
Gust Diaz Ordaz	SMSE_Gdiaz	1.04616	0.94	0.32344	0.13	0.024
San Juanico	SMSE_Sjuani	0.88295	0.95	0.29714	0.20	0.050
Cabo San Lucas	SMSE_CSL	2.22268	0.91	0.47145	0.19	0.057
Santa Rosalia	SMSE_SantaR	1.27369	0.94	0.35689	0.13	0.040
Sierra Laguna	SMSE_Slag	0.60661	0.96	0.24629	0.13	0.026
Cd Constitucion	SMSE_CdCons	0.58390	0.96	0.24164	0.14	0.030
La Paz	SMSE_LaPaz	0.89648	0.95	0.29941	0.15	0.029
Loreto	SMSE_Loreto	1.76413	0.92	0.42002	0.17	0.041
Sta Rosalia	SMSE_Srosa	1.68075	0.92	0.40997	0.17	0.042

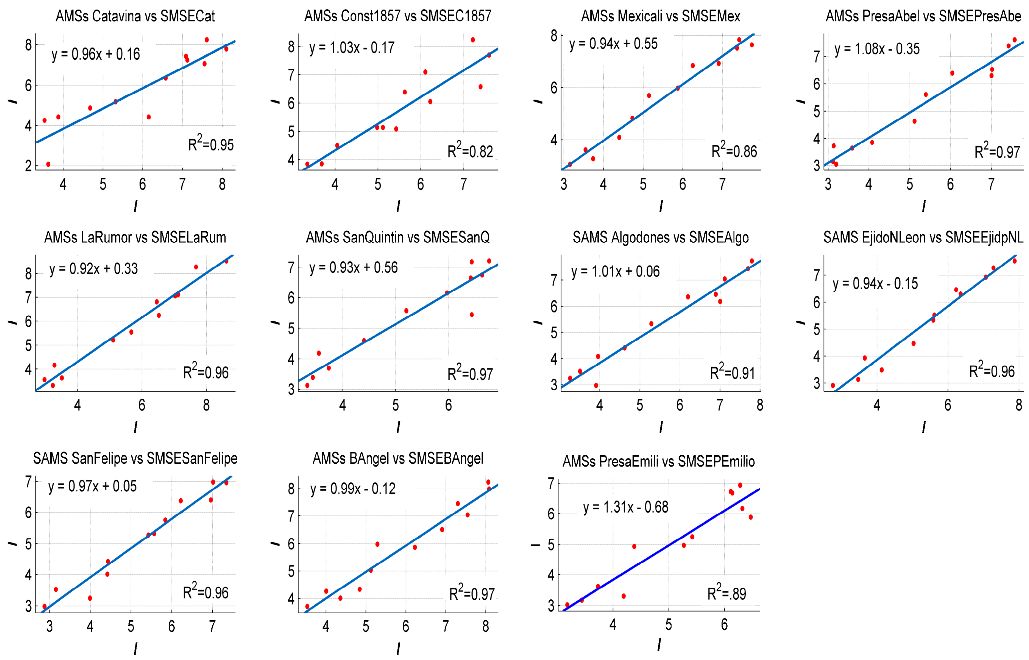

Figure 5. Monthly satellite versus measured data for each meteorological station in Baja California.

As we can see in Figure 5, linear fitting allows us to determine if we could use SMSE data for the assessment. The highest R-square value is 0.97 for AMSs PresaAbel, SanQuintin and BAngel, while the lowest R-square value is 0.82 corresponding to AMSs Const 1857. It is important to mention that SMSE data were extracted at the same geographic postion as the AMSs and SAMSs. In Baja California Sur, linear regression between AMSs and SAMSs versus SMSE data demonstrated that SMSE could be used to assess solar energy. In Figure 6, the highest value of R-square is 0.96 corresponding to SAMS CdConst and the lowest R-square 0.84 corresponds to AMS BahiaLore.

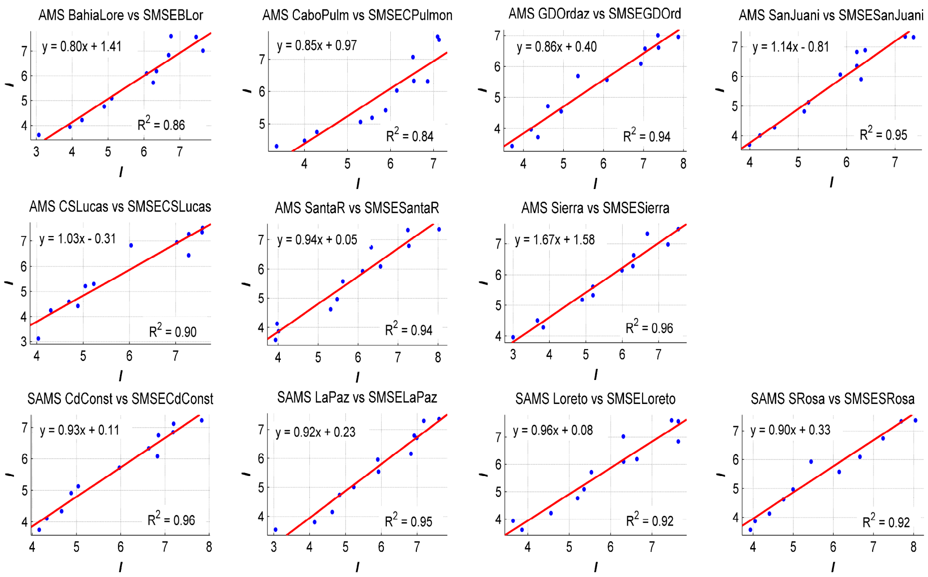

Figure 6. Monthly satellite vs. measured data for meteorological stations in Baja California Sur.

3.2. Solar Resource

3.2.1. Daily Pattern

An average day called daily pattern could help to identify how the irradiance is distributed at a site, and with it, it is possible to determine a model. This daily pattern is obtained grouping all the records at the same hour of all months. The results are represented in this work by two blocks of graphics, grouped by states (Baja California in Figure 7 and Baja California Sur in Figure 8), respectively. This pattern could be obtained as a result of the different methods applied.

The daily solar irradiance patterns for each meteorological station studied show the average during the day of irradiance. Figure 7 shows that Bahia Angeles, Cataviña, Mexicali, Presa Abelardo and San Felipe have more than 900 W/m^2. In Figure 8 the daily pattern behaved irregularly, as sensors lost a huge amount of data, even though it could find the pattern and the highest irradiance zones were Gustav Diaz Ordaz, San Juanico, Santa Rosal, Cd Constitucion, Santa Rosalia and Cabo San Lucas, all of which have over 900 W/m^2. However the other meteorological stations have good solar resources because the rest all have more than 800 W/m^2.

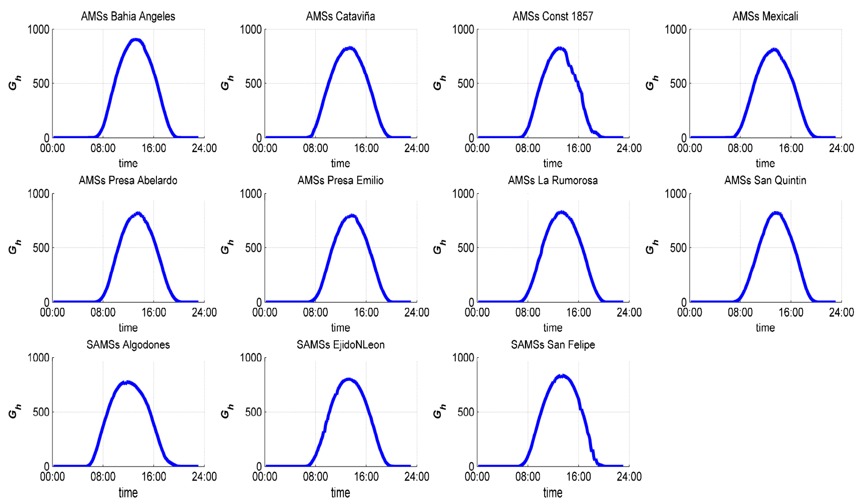

Figure 7. Daily irradiance patterns registered in Baja California.

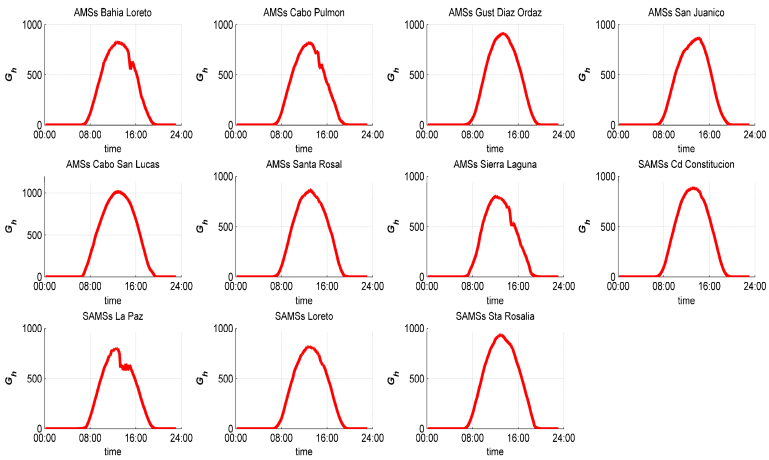

Figure 8. Daily irradiance patterns registered in Baja California Sur.

3.2.2. Solar Irradiation

Irradiation (I) was calculated using irradiance data transformed into energy. Table 3 shows these values. The information given in Table 3 describes the energy assessed by month and per meteorological station. June is the most energetic month, and La Rumorosa in this month has 8.7 kWh/m^2/day, followed by Cataviña, Bahia Angeles, Mexicali, Santa Rosal and Presa Abelardo with 8.6, 8.5, 8.3, 8.1 and 8.0 kWh/m^2/day, respectively. The annually irradiation range in the whole Peninsula is between 5.2 and 6.3 kWh/m^2/day.

Table 3. Monthly and annual irradiation per meteorological station.

Met. Station	Jan.	Feb.	Mar.	Apr.	May	Jun.	Jul.	Aug.	Sep.	Oct.	Nov.	Dec.	Annual
	(I) kWh/m^2/day												
Bahia Angeles	4.1	5.0	6.7	7.4	8.4	8.5	7.5	7.2	6.6	5.6	4.8	4.1	6.3
Catavina	4.2	4.8	6.4	7.4	8.4	8.6	7.9	7.2	6.5	5.1	4.5	3.6	6.2
Const. 1857	3.0	3.0	5.4	7.4	7.2	7.6	5.6	6.1	6.2	5.0	3.4	2.1	5.2
Mexicali	3.2	4.0	5.9	7.0	8.2	8.3	7.4	6.8	6.2	4.5	4.0	2.7	5.7
Presa Abelardo L.	3.6	4.4	5.2	6.4	7.2	8.0	7.5	7.2	5.8	4.9	3.4	3.2	5.6
Presa Emilio Lo	3.3	4.0	5.6	6.7	7.5	7.0	6.6	6.9	5.8	3.8	4.0	2.8	5.3
La Rumorosa	3.2	4.1	5.8	6.7	8.4	8.7	7.9	7.2	6.6	4.6	4.1	2.9	5.9
San Quintin	3.5	4.3	6.0	6.7	7.4	5.8	6.1	6.6	5.8	3.8	4.2	3.8	5.3
Algodones	3.8	4.4	5.8	6.8	7.1	6.3	6.6	5.7	5.6	4.4	3.6	1.9	5.2
Ejido Nvo. Leon	3.1	3.7	5.1	6.9	7.4	7.5	7.1	6.8	5.4	4.4	3.9	3.0	5.4
San Felipe	3.0	4.9	5.9	7.3	7.0	7.5	6.7	6.6	6.4	5.3	3.9	3.4	5.7
Bahia de Loreto	3.9	4.9	6.1	7.6	7.5	6.8	6.7	6.3	6.3	5.1	4.3	3.1	5.7
Cabo Pulmon	4.0	3.3	6.1	6.9	6.1	6.1	6.5	6.5	5.9	5.6	4.3	3.3	5.4
Gust Diaz Ordaz	4.3	5.4	6.2	7.3	8.1	7.8	7.4	7.2	6.5	5.6	4.2	3.8	6.2
San Juanico	4.5	5.1	6.4	6.9	7.3	7.0	6.6	6.4	6.2	5.4	4.7	3.8	5.9
Cabo San Lucas	4.8	5.5	6.3	6.7	7.3	7.6	7.3	6.7	5.9	5.9	4.5	4.5	6.1
Santa Rosal	4.5	5.5	6.6	7.7	8.4	8.1	7.5	6.8	6.0	5.2	4.2	3.7	6.2
Sierra Laguna	3.8	3.9	6.3	8.3	7.5	6.7	5.3	5.0	5.2	5.2	3.7	3.0	5.3
Cd Constitucion	4.3	4.9	6.5	7.3	8.1	7.9	7.4	6.7	6.2	5.6	4.9	4.1	6.2
La Paz	4.1	4.8	5.9	7.0	7.5	7.5	6.3	5.9	5.1	5.2	4.4	3.7	5.6
Loreto	3.8	4.2	5.0	6.5	6.1	6.3	6.2	6.0	5.8	5.5	4.4	2.7	5.2
Sta Rosalia	3.6	5.3	6.3	7.2	7.1	6.7	7.2	7.0	5.9	5.2	4.3	3.9	5.8

3.2.3. Solar Maps

The urban zones with higher solar resource are represented in maps, this is the reason that only are represented the areas where there are urban zones. Figures 9–11 show monthly solar resources and Figure 12 represents the annual solar resource in the Peninsula. The Baja California Peninsula is considered a desert zone; also, it can extract some tendencies from these irradiation maps. Topography effects are localized in some regions, e.g., Figure 10 shown that May and June present the highest mean solar resource range over 8.1 kWh/m^2/day at the south of the Peninsula, however at the north the irradiation presents lower values since 5.6 kWh/m^2/day to over 8.1 kWh/m^2/day.

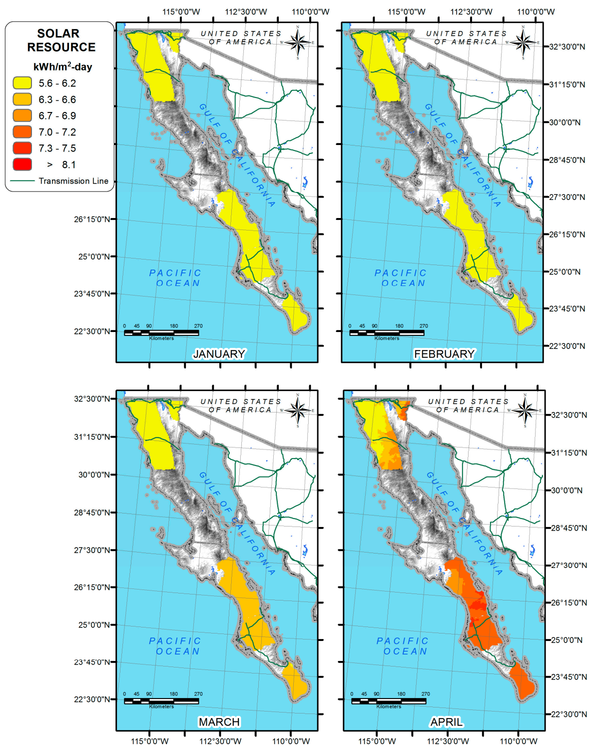

Figure 9. Irradiation on the Baja California Peninsula, January to April.

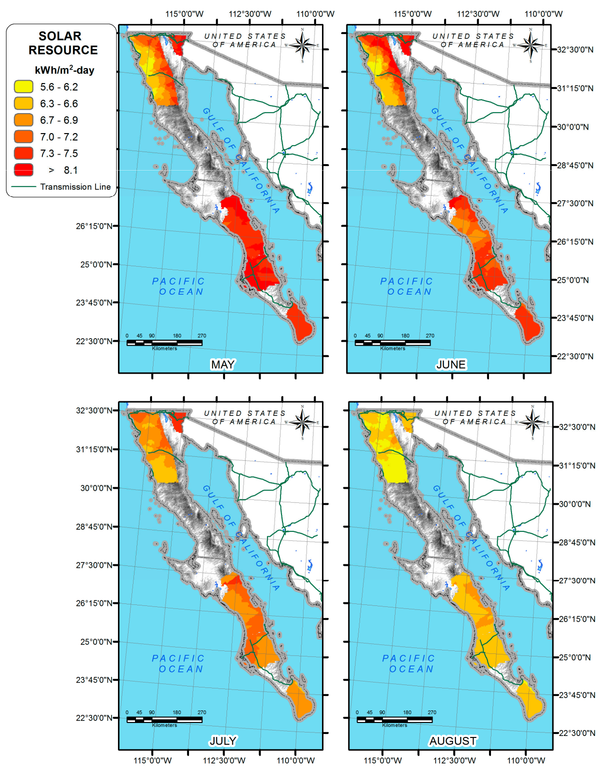

Figure 10. Irradiation at the Baja California Peninsula, May to August.

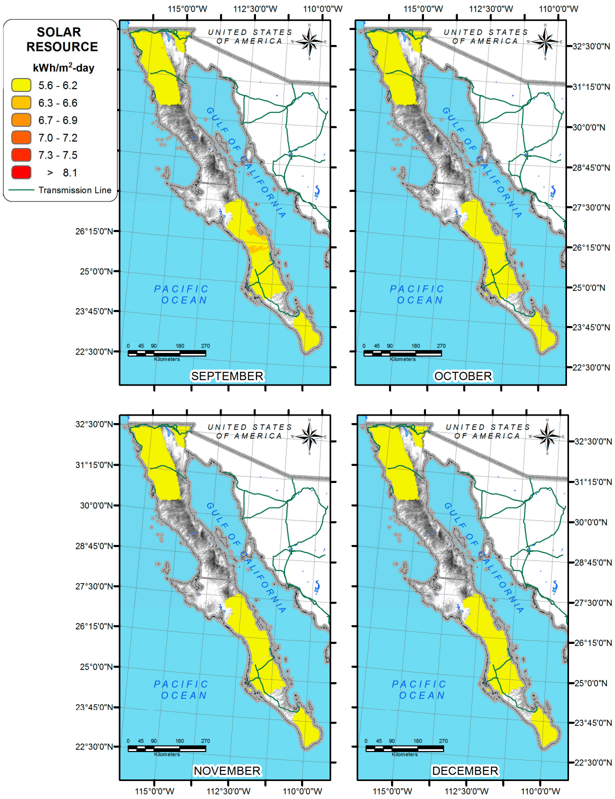

Figure 11. Irradiation at the Baja California Peninsula, September to December.

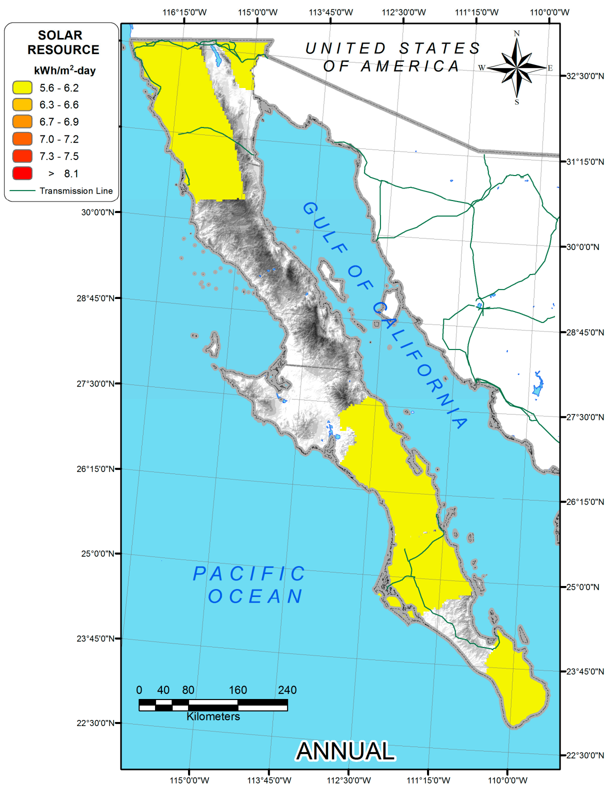

Figure 12. Annual Irradiation at the Baja California Peninsula.

The Peninsula shows low temporal and spatial variability of global irradiation, according to Figures 9 and 11 January and February and September, October, November and December are the months with lower solar resources and one can see the tendency of the date, whereby even though these months have the lowest resource, its range is still between 5.6 kWh/m^2/day and 6.2 kWh/m^2/day. The annual map, Figure 12, indicates that the yearly range of solar resource over the Peninsula is between 5.6 kWh/m^2/day and 6.2 kWh/m^2/day. Considering the urban areas, total solar irradiation reaching the Peninsula is about 447×10^6 kWh, which represents around 447 times the total yearly energy consumption of Baja California Peninsula. Only urban communities zones are represented, as the rest of the peninsula is rural, and for this reason only some zones are mapped.

4. Discussion

This study presents the magnitude ranges of solar energy in the Baja California Peninsula, which almost 2.4% of urban communities are not electrified [16]. According to previous studies, the average solar resource in the whole of Mexico is 6.5 kWh/m^2/day [12]; in this work the average for the whole Peninsula was 5.7 kWh/m^2/day (see Table 3).

Daily patterns show the solar irradiance in each studied station; in Baja California (Figure 7) Bahia Angeles, Constitucion 1857 and La Rumorosa have more than 900 W/m^2. Cabo San Lucas was the only zone with more than 1000 W/m^2 in an average day, but Gustav Diaz Ordaz, San Juanico and Santa Rosalia all show more than 900 W/m^2 (Figure 8).

If the Peninsula is analyzed separately, on the one hand Baja California presents in the north the highest value (over 8.1 kWh/m^2/day) in May and June, as is shown in Figure 10, while the rest of Baja California during the same months has a range between 5.6 kWh/m^2/day to 7.5 kWh/m^2/day. Baja California Sur in May (Figure 10) has a solar resource between 7 kWh/m^2/day to more than 8.1 kWh/m^2/day in the whole analyzed territory, and in June its range is 6.7 kWh/m^2/day to 7.2 kWh/m^2/day. The whole Peninsula has more than 5.6 kWh/m^2/day during the whole year. It is important to clarify that maps represent only the solar resources in urban zones, blank spaces are not considered to this work.

5. Conclusions

This work has presented the first downscaled solar atlas of urban areas of the Baja California Peninsula, using satellite and measured data. Satellite data were linearly fitted versus AMSs and SAMSs data to compare them, and the linear regression results gave an R-square value between 0.82 and 0.97 (see Table 2) which gave us confidence to continue the study. Furthermore, the process could be computed again in the futures better spatial definition. Both *MAE* and bias are close to 0, and it is important to mention that SMSE data were compared with fixed data from meteorological stations. Daily patterns were calculated per meteorological station, and these patterns could give an idea of the amount of irradiance per typical day in the Peninsula.

Finally, we have exposed global irradiation monthly maps of the Baja California Peninsula. These maps showed spatial variability across the Peninsula, and in the North, this could be due to the topography. The months with higher solar resource are May and June with a irradiation over 8.1 kWh/m^2/day and the months with lower solar resource are January, February, September, October, November and December because the range is between 5.6 kWh/m^2/day and 6.2 kWh/m^2/day.

At present, energy supply and electrification is one of the most important challenges in Mexico. The present government has done structural reforms including opening the energy industry sector to private investors; this could help the population's development. With this study, we can identify the zones with high solar resource to help develop the solar industry.

Acknowledgments: Authors would like to acknowledge to NMS of Mexico and SMSE for providing data.

Author Contributions: Alberto-Jesús Perea-Moreno and Quetzalcoatl Hernandez-Escobedo conceived and designed the experiments; Alberto-Jesús Perea-Moreno and Quetzalcoatl Hernandez-Escobedo performed the experiments analyzed the data; Alberto-Jesús Perea-Moreno and Quetzalcoatl Hernandez-Escobedo wrote the paper.

Conflicts of Interest: The authors declare no conflict of interest.

Abbreviations

The following abbreviations are used in this manuscript:

AMS	Automatic Meteorological Stations
SAMS	Synoptic Automatic Meteorological Station
NMS	National Meteorological System of Mexico
SMSE	Surface and Meteorology Energy System
GIS	Geographic Information System
GWh	Gigawatts-hour
MW	Megawatt
PV	Photovoltaic
CSP	Concentrated Solar Power
MWh	Megawatt-hour
RMSE	Root Mean Square Error
SS_E	Error Sum of Squares
SS_R	Regresion Sum of Squares
SS_T	Total Sum of Squares
TMY	Typical Meteorological Year

References

1. International Energy Agency (IEA). Available online: http://energyatlas.iea.org (accessed on 4 February 2016).
2. Castellano, N.N.; Gázquez Parra, J.A.; Valls-Guirado, J.; Manzano-Agugliaro, F. Optimal displacement of photovoltaic array's rows using a novel shading model. *Appl. Energy* **2015**, *144*, 1–9. [CrossRef]
3. Hasanuzzaman, M.; Malek, A.B.M.A.; Islam, M.M.; Pandey, A.K.; Rahim, N.A. Global advancement of cooling technologies for PV systems: A review. *Sol. Energy* **2016**, *137*, 25–45. [CrossRef]
4. De la Tour, A.; Glachant, M.; Meniere, Y. Innovation and international technology transfer: The case of the Chinese photovoltaic industry. *Energy Policy* **2011**, *39*, 761–770. [CrossRef]
5. The International Renewable Energy Agency (IRENA). Renewable Power Generation Costs. Available online: http://www.IRENA.org/DocumentDownloads/Publications/IRENA_RE_Power_Costs_2014_report.pdf (accessed on 30 September 2016).
6. Bloomberg. The Way Humans Get Electricity Is About to Change Forever, Bloomberg Business. Available online: http://www.bloomberg.com/news/articles/2015-06-23/the-way-humans-get-electricity-is-about-to-change-forever (accessed on 30 September 2016).
7. Ondraczek, J.; Komendantova, N.; Patt, A. WACC the dog: The effect of financing costs on the levelized cost of solar PV power. *Renew. Energy* **2015**, *75*, 888–898. [CrossRef]
8. Ryan, L.; Dillon, J.; Monaca, S.L.; Byrne, J.; O'Malley, M. Assessing the system and investor value of utility-scale solar PV. *Renew. Sustain. Energy Rev.* **2016**, *64*, 506–517. [CrossRef]
9. Zhu, H.; Li, X.; Sun, Q.; Nie, L.; Yao, J.; Zhao, G. A power prediction method for photovoltaic power plant based on wavelet decomposition and artificial neural networks. *Energies* **2016**, *9*, 11. [CrossRef]
10. Secretaria de Energia (SENER). Available online: http://sie.energia.gob.mx (accessed on 4 February 2016).
11. Comision Nacional para el Uso Eficiente de la Energia (Conuee). Available online: http://www.conuee.gob.mx (accessed on 20 May 2016).
12. Hernandez-Escobedo, Q.; Rodriguez-Garcia, E.; Saldana-Flores, R.; Garcia-Fernandez, A. Manzano-Agugliaro, F. Solar energy resource assessment in the Mexican states along the Gulf of Mexico. *Renew Sust. Energy Reviews.* **2015**, *43*, 216–238. [CrossRef]
13. Sosa-Tinoco, I.; Peralta-Jaramillo, J.; Otero-Casal, C.; Lopez-Aguera, A.; Miguez-Machi, G.; Rodriguez-Cabo, I. Validation of a global horizontal irradiation assessment from a numerical weather prediction model in south of Sonora-Mexico. *Renew. Energy* **2016**, *90*, 105–113. [CrossRef]

14. The World Bank. Available online: http://data.worldbank.org/indicator/SI.POV.RUHC (accessed on 5 February 2016).
15. Comision Federal de Electricidad (CFE). Available online: http://cfe.gob.mx (accessed on 5 February 2016).
16. Instituto Nacional de Estadistica y Geografia (INEGI). Available online: www.inegi.org.mx (accessed on 5 February 2016).
17. Energetic Information System, Mexico. Available online: http://cfe.gob.mx (accessed on 4 April 2016).
18. Energetic Transition Law (ETL). Available online: http://dof.gob.mx (accessed on 7 February 2016).
19. National Meteorological Service Mexico (NMS). Available online: http://smn.gob.mx (accessed on 4 January 2016).
20. Surface Meteorology and Solar Energy (SMSE). Available online: https://eosweb.larc.nasa.gov/sse/ (accessed on 7 January 2016).
21. Polo, J.; Zarzalejo, L.F.; Cony, M.; Navarro, A.A.; Marchante, R.; Martin, L. Solar radiation estimations over India using Meteosat satellite images. *Sol. Energy* **2011**, *85*, 2395–2406. [CrossRef]
22. Zelenka, A.; Perez, R.; Seals, R.; Renne, D. Effective accuracy of satellite-derived hourly irradiations. *Theor. Appl. Climatol.* **1999**, *62*, 199–207. [CrossRef]
23. Vignola, F.; Harlan, P.; Perez, R.; Kmiecik, M. Analysis of satellite derived beam and global solar radiation data. *Sol. Energy* **2007**, *81*, 768–772. [CrossRef]
24. Pedro, H.T.C.; Coimbra, C.F.M. Assessment of forecasting techniques for solar power production with no exogenous inputs. *Sol. Energy* **2012**, *86*, 2017–2028. [CrossRef]
25. Lee, K.; Yoo, H.; Levermore, G. Quality control and estimation hourly solar irradiation on inclined surfaces in South Korea. *Renew. Energy* **2013**, *57*, 190–199. [CrossRef]
26. Maghrabi, A.H. Parameterization of a simple model to estimate monthly global solar radiation based on meteorological variables, and evaluation of existing solar radiation models for Tabouk, Saudi Arabia. *Energy Convers. Manag.* **2009**, *50*, 1754–2760. [CrossRef]
27. Wu, G.; Liu, Y.; Wang, T. Methods and strategy for modeling daily global solar radiation with measured meteorological data—A case study in Nanchang station, China. *Energy Convers. Manag.* **2007**, *48*, 2447–2452. [CrossRef]
28. User's Manual for TMY2s Typical Meteorological Years. Available online: http://rredc.nrel.gov/solar/pubs/tmy2/pdfs/tmy2man.pdf (accessed on 1 November 2016).